UC Irvine
UC Irvine Previously Published Works

Title

β-Hairpin Alignment Alters Oligomer Formation in Aβ-Derived Peptides.

Permalink

https://escholarship.org/uc/item/0g5169f9

Journal

Biochemistry, 63(2)

Authors

Ruttenberg, Sarah

Kreutzer, Adam

Truex, Nicholas

et al.

Publication Date

DOI

Peer reviewed

Article

β-Hairpin Alignment Alters Oligomer Formation in Aβ-Derived Peptides

Sarah M. Ruttenberg, Adam G. Kreutzer, Nicholas L. Truex, and James S. Nowick*

Cite This: Biochemistry 2024, 63, 212−218

Read Online

ACCESS | Metrics & More | Article Recommendations | Supporting Information

ABSTRACT: Amyloid-β (Aβ) forms heterogeneous oligomers, which are implicated in the pathogenesis of Alzheimer's disease (AD). Many Aβ oligomers consist of β-hairpin building blocks—Aβ peptides in β-hairpin conformations. β-Hairpins of Aβ can adopt a variety of alignments, but the role that β-hairpin alignment plays in the formation and heterogeneity of Aβ oligomers is poorly understood. To explore the effect of β-hairpin alignment on the oligomerization of Aβ peptides, we designed and studied two model peptides with two different β-hairpin alignments. Peptides $A\beta m_{17-36}$ and $A\beta m_{17-35}$ mimic two different β-hairpins that Aβ can form, the $A\beta_{17-36}$ and $A\beta_{17-35}$ β-hairpins, respectively. These hairpins are similar in composition but differ in hairpin alignment, altering the facial arrangements of the side chains of the residues that they contain. X-ray crystallography and SDS-PAGE demonstrate that the difference in facial arrangement between these peptides leads to distinct oligomer formation. In the crystal state, $A\beta m_{17-36}$ forms triangular trimers that further assemble to form hexamers, while $A\beta m_{17-35}$ forms tetrameric β-barrels. In SDS-PAGE, $A\beta m_{17-36}$ assembles to form a ladder of oligomers, while $A\beta m_{17-35}$ either assembles to form a dimer or does not assemble at all. The differences in the behavior of $A\beta m_{17-36}$ and $A\beta m_{17-35}$ suggest β-hairpin alignment as a source of the observed heterogeneity of Aβ oligomers.

L V F F A E D / V M L G I I A   L V F F A E D / M L G I I A G
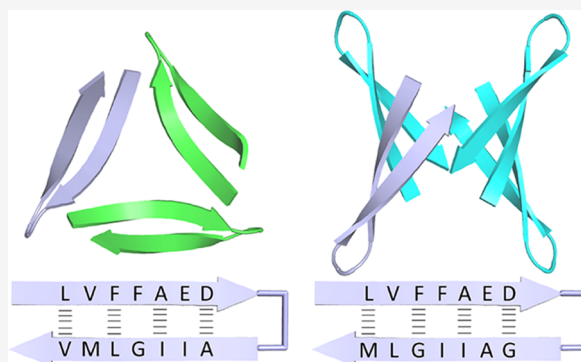
INTRODUCTION

Amyloid-β (Aβ) is intrinsically disordered and can adopt myriad conformations, including β-sheets, α-helices, and a variety of β-hairpins.[1−18] These secondary structures can direct the formation of toxic Aβ assemblies implicated in Alzheimer's disease (AD).[4,6,9,11,12,15−18] Several studies have demonstrated that toxic Aβ oligomers consist of β-hairpin building blocks.[4,6,9,12,19] Multiple β-hairpins have been reported for Aβ that differ in the alignment of the β-strands and the residues they contain.[1,4,6−13,18,19] The role that β-hairpin alignment plays in the formation and heterogeneity of oligomers of Aβ is poorly understood. Atomic-level analysis of these oligomers is necessary to better understand the molecular basis of AD, but the transience of Aβ oligomers makes their characterization difficult.

To better study these elusive Aβ oligomers, our laboratory has developed peptide model systems consisting of conformationally constrained β-hairpin peptides derived from Aβ.[20−27] These model systems have provided a variety of high-resolution structures of oligomeric assemblies that cannot be achieved from oligomers formed by Aβ itself. In the current study, we use two similar model peptides to explore the effect of β-hairpin alignment on the assembly of peptides derived from Aβ. $A\beta m_{17-36}$ and $A\beta m_{17-35}$ mimic two different β-hairpins that Aβ can form, the $A\beta_{17-36}$ and $A\beta_{17-35}$ β-hairpins, respectively.[13,18,19]

$A\beta m_{17-36}$ and $A\beta m_{17-35}$ differ in the alignment of the β-strands that comprise each peptide. In both peptides, residues 17−23 constitute one of the β-strands. In $A\beta m_{17-36}$, residues 30−36 constitute the other β-strand, while in $A\beta m_{17-35}$, residues 29−35 constitute the other β-strand (Figure 1). This difference results in a different alignment of the peptide strands, with the bottom strand of $A\beta m_{17-36}$ shifted by one amino acid toward the C-terminus in comparison to $A\beta m_{17-35}$. Thus, Leu_{17} is across from Val_{36} in $A\beta m_{17-36}$, while Leu_{17} is across from Met_{35} in $A\beta m_{17-35}$. This shift changes the hydrogen-bonded pairs of the residues within the hairpin as well as the surface on which the side chains are displayed. The change in facial arrangement is illustrated in Figure 1, with the even-numbered side chains (green) displayed on the "top" face in $A\beta m_{17-36}$ and the "bottom" face in $A\beta m_{17-35}$.
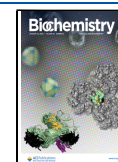
Notably, the chemical compositions of $A\beta m_{17-36}$ and $A\beta m_{17-35}$ are almost identical—$A\beta m_{17-36}$ contains Val_{36} whereas $A\beta m_{17-35}$ contains Gly_{29}. The similarity of $A\beta m_{17-36}$
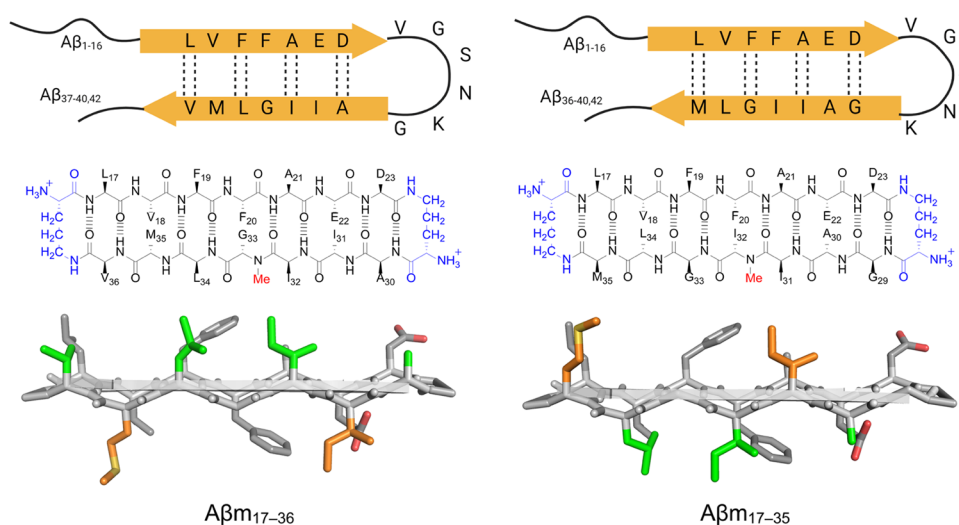
Figure 1. Cartoon representations of the $A\beta_{17-36}$ and $A\beta_{17-35}$ hairpins (top). Chemical drawings (middle) and cartoon representations (bottom) of $A\beta m_{17-36}$ and $A\beta m_{17-35}$. In the chemical drawings, the δ-linked ornithine turn units are shown in blue, and the N-methyl group is shown in red. In the cartoon representations, the residues in $A\beta m_{17-35}$ are colored to match those in $A\beta m_{17-36}$, indicating the differences between the faces of $A\beta m_{17-36}$ and $A\beta m_{17-35}$.

and $A\beta m_{17-35}$ makes them good candidates for exploring how β-hairpin alignment, and thus the facial arrangement of residues, affects oligomeric assembly. In this study, we compare $A\beta m_{17-36}$ and $A\beta m_{17-35}$ and demonstrate that the alignment of the β-hairpin can affect the assembly of peptides derived from $A\beta$.

RESULTS AND DISCUSSION

Design of the Model System. $A\beta m_{17-36}$ and $A\beta m_{17-35}$ are cyclic hexadecapeptides consisting of two heptapeptide β-strands ($A\beta_{17-23}$ and $A\beta_{30-36}$ or $A\beta_{29-35}$) connected by two δ-linked ornithine turn units that promote a β-hairpin-like conformation. The peptides also contain an N-methyl group on Gly_{33} ($A\beta m_{17-36}$) or Ile_{32} ($A\beta m_{17-35}$) to attenuate aggregation through the formation of intermolecular hydrogen bonds. These features facilitate the formation of well-defined oligomers that, unlike oligomers of full-length $A\beta$, are amenable to high-resolution structural characterization through X-ray crystallography.

$A\beta m_{17-36}$ is designed to display the side chains of Val_{36}, Leu_{34}, Ile_{32}, and Ala_{30} on the same face of the β-hairpin as the side chains of Leu_{17}, Phe_{19}, Ala_{21}, and Asp_{23} (the LFAD face). The side chains of Met_{35}, N-methyl-Gly_{33}, and Ile_{31}, as well as the side chains of Val_{18}, Phe_{20}, and Glu_{22}, are in turn displayed on the opposite face (the VFE face). $A\beta m_{17-35}$ is designed to display the side chains of Met_{35}, Gly_{33}, Ile_{31}, and Gly_{29} on the LFAD face and the side chains of Leu_{34}, N-methyl-Ile_{32}, and Ala_{30} on the VFE face. Figure 1 illustrates these differences through the colors of the side chains (green and orange). While both peptides primarily consist of hydrophobic residues, the differences between the faces of $A\beta m_{17-36}$ and $A\beta m_{17-35}$ lead to the formation of different oligomeric assemblies.

Assembly by SDS-PAGE. $A\beta m_{17-36}$ and $A\beta m_{17-35}$ were subjected to sodium dodecyl sulfate-polyacrylamide gel electrophoresis (SDS-PAGE) to evaluate their propensity to oligomerize. When a 200 μM solution of $A\beta m_{17-36}$ is subjected to SDS-PAGE and visualized by silver staining, a ladder of seven bands is observed (Figure 2). The bands appear to be evenly separated by about 2 kDa, which is consistent with the molecular weight of the monomer (1.76 kDa). The lowest
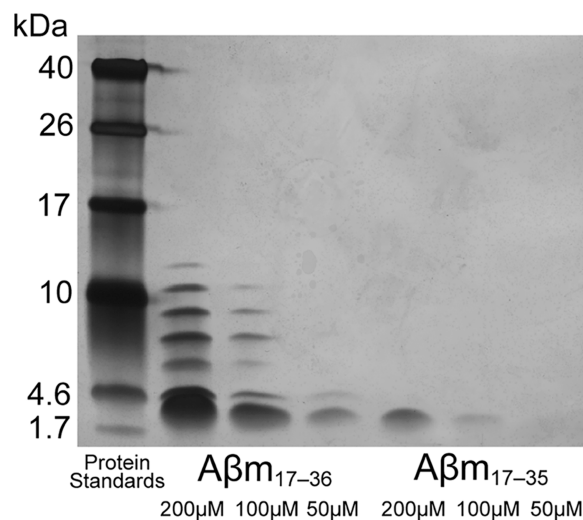

Figure 2. Silver-stained SDS-PAGE gel of $A\beta m_{17-36}$ and $A\beta m_{17-35}$.

molecular weight band corresponds to either monomer or dimer, and the subsequent bands correspond to either dimer through heptamer or trimer through octamer. The ladderlike appearance suggests that the oligomers are formed by sequential addition of $A\beta m_{17-36}$ monomers. The intensities of the bands indicate that the smallest species (monomer or dimer) predominates and that the oligomers corresponding to the second, fourth, fifth, and sixth bands may be more stable than those corresponding to the third. Fewer bands are observed with decreasing concentration, suggesting that oligomer formation is dependent on concentration. Alternatively, the larger oligomers may still be present at lower concentrations but not abundant enough to reach the sensitivity limit of the silver stain.

To our knowledge, the periodic ladderlike oligomerization exhibited by $A\beta m_{17-36}$ has not been observed for other $A\beta$ peptides in SDS-PAGE. $A\beta_{1-42}$ typically exhibits prominent monomer, trimer, and tetramer bands in SDS-PAGE, while $A\beta_{1-40}$ typically exhibits predominantly a monomer band.[28−30] Ladders of oligomers are observed in SDS-PAGE when $A\beta_{1-40}$
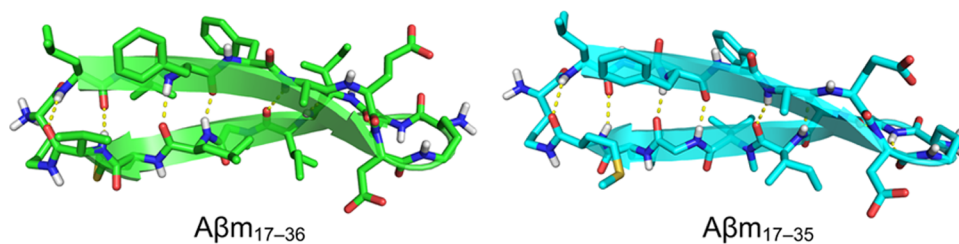
Figure 3. X-ray crystallographic structures of representative monomers of Aβm$_{17-36}$ and Aβm$_{17-35}$ (PDB 8GJD and 8GJC). Aβm$_{17-36}$ contains 16 unique molecules in the asymmetric unit; Aβm$_{17-35}$ contains 2 unique molecules in the asymmetric unit.
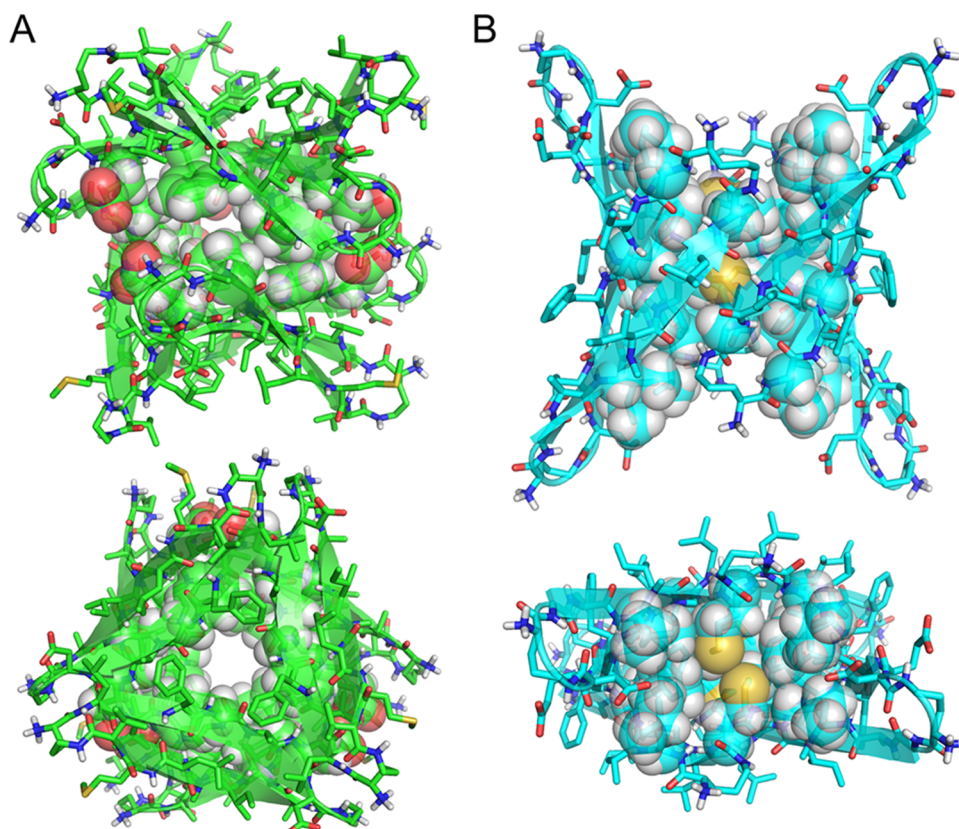

Figure 4. X-ray crystallographic structure of (A) the hexamer formed by Aβm$_{17-36}$ and (B) the tetramer formed by Aβm$_{17-35}$. Side chains of residues in the hydrophobic cores of the assemblies are shown as spheres to illustrate packing. Assemblies are shown from a "side" view (top) and then rotated 90 to show a "top" view (bottom).

or Aβ$_{1-42}$ are subjected to photoinduced cross-linking of unmodified proteins (PICUP).[28,29] Our laboratory has also observed a ladder of oligomers upon TCEP treatment of an Aβ$_{1-42}$ peptide containing an intramolecular disulfide bond.[31,32]

In contrast to Aβm$_{17-36}$, Aβm$_{17-35}$ migrates as a single diffuse band at molecular weights consistent with a monomer or dimer in SDS-PAGE (Figure 2). Aβm$_{17-35}$ exhibits fainter bands than Aβm$_{17-36}$ at the same concentrations. Staining with Bio-Rad fluorescent stains Flamingo and Oriole also showed slightly weaker bands for Aβm$_{17-35}$ compared to Aβm$_{17-36}$ (data not shown). The decreased intensity of Aβm$_{17-35}$ with both silver staining and fluorescent stains might reflect a greater propensity of Aβm$_{17-35}$ to diffuse out of the gel during the staining process or lower solubility of Aβm$_{17-35}$ leading to poorer penetration into the gel.

X-ray Crystallography. Aβm$_{17-36}$ and Aβm$_{17-35}$ both proved to be amenable to structural elucidation by X-ray

crystallography (Figure 3). Aβm$_{17-36}$ afforded crystals under conditions used previously for a homologue containing ornithine in place of Met$_{35}$ (HEPES buffer and Jeffamine M-600).[33] Aβm$_{17-35}$ afforded crystals from a buffer consisting of bicine and Trisma and a mixture of ethylene glycol oligomers. Diffraction data for crystals of Aβm$_{17-36}$ were collected to 2.05 Å in-house on a Rigaku Micromax-007HF X-ray diffractometer equipped with a copper anode. Diffraction data for crystals of Aβm$_{17-35}$ were collected to 1.52 Å on the synchrotron at the Advanced Light Source at Lawrence Berkeley National Laboratory. The X-ray crystallographic phases of Aβm$_{17-36}$ were solved by soaking the crystals in potassium iodide to incorporate iodide ions into the crystal lattice and then performing single-wavelength anomalous diffraction (SAD) phasing. The X-ray crystallographic phases of Aβm$_{17-35}$ were solved using molecular replacement with an all-alanine model of a related β-hairpin peptide as a search model (PDB 5W4H).[34]
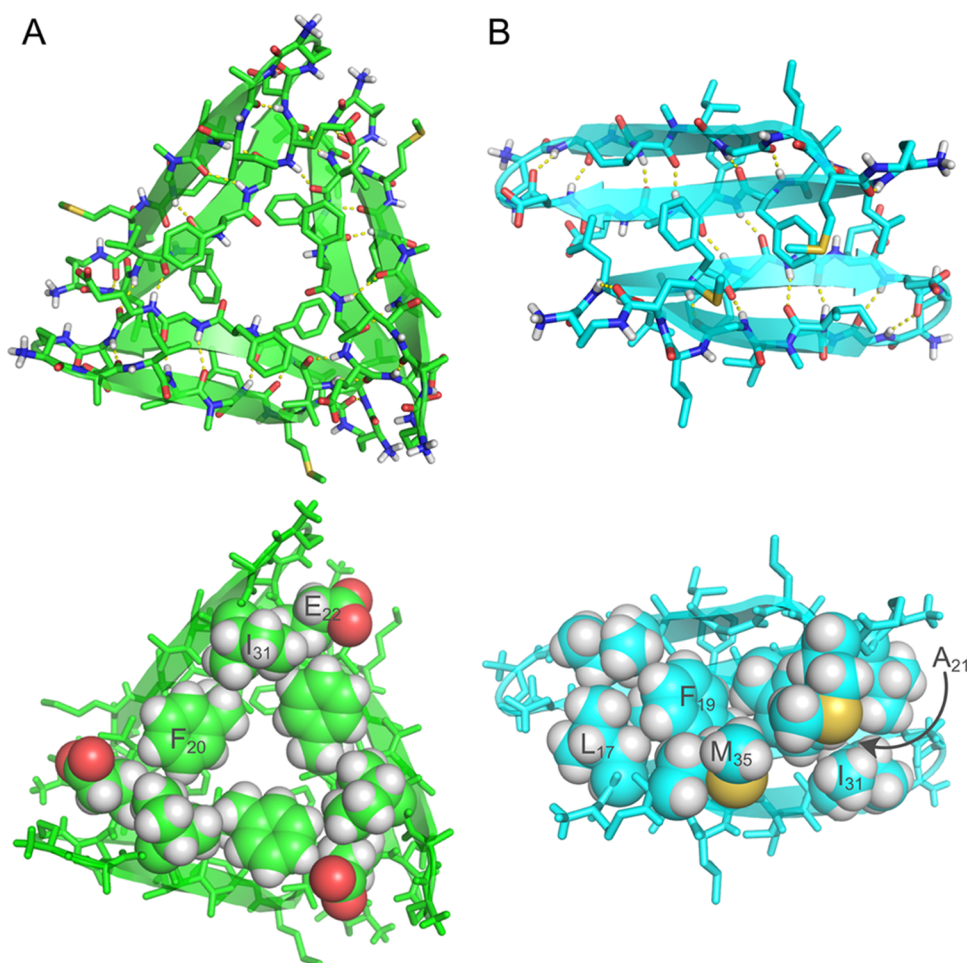
Figure 5. X-ray crystallographic structures of (A) a trimer formed by Aβm$_{17-36}$ and (B) an antiparallel dimer formed by Aβm$_{17-35}$. Hydrogen bonds within the structures are shown by yellow dashed lines (top). The side chains of residues that pack into the hydrophobic core of the hexamer formed by Aβm$_{17-36}$ and the tetramer formed by Aβm$_{17-35}$ are shown as spheres (bottom). These residues are labeled on one monomer within each structure. Ala$_{21}$ in the dimer of Aβm$_{17-35}$ is mostly hidden behind Phe$_{19}$ and Met$_{35}$ of the adjacent molecule of Aβm$_{17-35}$.

Aβm$_{17-36}$ and Aβm$_{17-35}$ form different oligomers in the crystal state. The X-ray crystallographic structure of Aβm$_{17-36}$ contains 16 molecules of Aβm$_{17-36}$ in the asymmetric unit. Each of the molecules folds to form a twisted β-hairpin, and variation between monomers is minimal, consisting mainly of Met$_{35}$ and Leu$_{34}$ rotamers. In the crystal lattice, Aβm$_{17-36}$ assembles to form trimers, which loosely pack into hexamers (Figure 4A). The X-ray crystallographic structure of Aβm$_{17-35}$ contains two molecules of Aβm$_{17-35}$ in the asymmetric unit. Both molecules fold to form twisted β-hairpins, and variation between the two monomers is minimal, consisting mainly of Met$_{35}$ rotamers. The different Met$_{35}$ rotamers likely aid in maximizing hydrophobic packing within the crystal lattice. In the crystal lattice, both molecules of Aβm$_{17-35}$ assemble to form tetrameric β-barrels or cylindrins[35] (Figure 4B).

The trimers formed by Aβm$_{17-36}$ consist of three β-hairpins in a triangular assembly with a cavity at the center of the triangle (Figure 5A). Phe$_{20}$ and Phe$_{19}$ sit on opposite faces at the center of the trimer surrounding this cavity. The trimer is stabilized by hydrophobic packing of residues on both faces and by intermolecular hydrogen bonding between the backbones of Val$_{18}$ and Glu$_{22}$ at each corner. Two trimers further pack together on the VFE face to form a hexamer. Although the hexamer is not stabilized by hydrogen bonds between the component trimers, it is stabilized by bridging

water molecules that hydrogen bond to both trimers. The side chains of residues Phe$_{20}$, Glu$_{22}$, and Ile$_{31}$ form the hydrophobic core of the hexamer, with the carboxyl groups of Glu$_{22}$ sitting at the corners. Although Met$_{35}$ and Gly$_{33}$ also sit on the VFE face of Aβm$_{17-36}$, neither appears to contribute to the packing of the trimer or hexamer.[36] The remaining side chains sit outside of the hydrophobic core of the hexamer.

The tetramers formed by Aβm$_{17-35}$ consist of four β-hairpins arranged around a central axis to form a β-barrel. The tetramer can be viewed as a dimer of dimers in which two monomers assemble to form an antiparallel dimer (Figure 5B), and two antiparallel dimers further assemble to form the tetramer. The hydrophobic side chains of the LFAD face comprise the core of the tetramer. The side chains of Phe$_{19}$ and Met$_{35}$ lie at the center of the hydrophobic core and are buttressed by the side chains of Leu$_{17}$, Ala$_{21}$, and Ile$_{31}$. The absence of a side chain at Gly$_{33}$ facilitates the tight packing of these hydrophobic side chains in a fashion similar to that previously reported for a cylindrin comprising three β-hairpins from αB crystallin.[35] The charged residues Glu$_{22}$ and Asp$_{23}$ sit on the solvent-exposed ends of the Aβm$_{17-35}$ cylindrin away from the hydrophobic core. Intermolecular hydrogen bonds between the monomer subunits further stabilize the tetramer. The backbones of the Phe$_{20}$ residues hydrogen bond to each other at the interfaces between monomers within the dimers. The backbones of the

Leu$_{34}$ residues hydrogen bond to each other at the interfaces between the dimers.

Although both the hexamer of Aβm$_{17-36}$ and the tetramer of Aβm$_{17-35}$ are stabilized by hydrophobic packing, this packing occurs on opposite faces of the peptides. The hexamer of Aβm$_{17-36}$ packs on the VFE face, even though the LFAD face displays three more hydrophobic side chains (Val$_{18}$, Phe$_{20}$, Ile$_{31}$, and Met$_{35}$ vs Leu$_{17}$, Phe$_{19}$, Ala$_{21}$, Ala$_{30}$, Ile$_{32}$, Leu$_{34}$, and Val$_{36}$). Additional intermolecular contacts in the lattice involving Leu$_{17}$ and Val$_{36}$ may promote packing of the trimers on the less hydrophobic VFE face. The relatively loose packing of the trimers within the hexamer suggests that the trimer is the primary oligomeric building block in the crystal lattice. To this end, the trimer is stabilized by extensive packing of three sets of hydrophobic side chains in its center (Leu$_{17}$, Phe$_{19}$ Phe$_{20}$, Ala$_{21}$, Ile$_{31}$, and Leu$_{34}$).

The Aβm$_{17-35}$ tetramer packs on the LFAD face rather than the VFE face. The two faces each display the same number of hydrophobic side chains (Leu$_{17}$, Phe$_{19}$, Ala$_{21}$, Ile$_{31}$, and Met$_{35}$ vs Val$_{18}$, Phe$_{20}$, Ala$_{30}$, Ile$_{32}$, and Leu$_{34}$). Packing on the LFAD face may result from better self-complementarity of this face, permitting tighter hydrophobic packing. No major hydrophobic interactions are observed between the tetramers in the lattice, despite the exterior of each tetramer presenting multiple hydrophobic side chains. Although the tetramers pack together in the lattice, the packing interactions do not appear to lead to well-defined higher-order assemblies.

The assemblies observed for Aβm$_{17-36}$ and Aβm$_{17-35}$ in the crystal state do not match the assemblies observed in SDS-PAGE. These differences likely result from the different experimental conditions required for SDS-PAGE and crystallization.[53] SDS-PAGE is run at micromolar concentrations in a pH 6.8 Tris loading buffer containing 2% glycerol. Crystallization occurs at millimolar concentrations at pH 6.75 and pH 8.5 for Aβm$_{17-36}$ and Aβm$_{17-35}$, respectively. The varied behaviors of Aβm$_{17-36}$ and Aβm$_{17-35}$ across different techniques are reminiscent of that of full-length Aβ peptides, for which assembly is highly dependent on experimental conditions.[37−52] Peptide concentration, the presence of detergents or lipids, pH, and temperature, among other factors, can direct, alter, induce, or inhibit assembly in full-length Aβ peptides.[37−52]

Aβm$_{17-36}$ and Aβm$_{17-35}$ mimic just two of the many conformations that full-length Aβ can form. In this paper, X-ray crystallography and SDS-PAGE demonstrate that the alignment of the β-strands within an Aβ-derived β-hairpin affects how the peptide oligomerizes. The range of assemblies Aβm$_{17-36}$ and Aβm$_{17-35}$ form under different conditions exemplifies how β-hairpin assembly can be affected by environment and provides insight into the factors that drive the oligomerization of Aβ peptides. The current study provides evidence that β-hairpin formation, along with environmental variation, can contribute to Aβ oligomer heterogeneity. While the heterogeneity of Aβ oligomers is still an obstacle to understanding the molecular basis of AD, this study illustrates how small changes in the folding of the component Aβ monomer subunits can have profound effects on Aβ oligomer structure and assembly.

■ MATERIALS/EXPERIMENTAL METHODS

Peptides Aβm$_{17-36}$ and Aβm$_{17-35}$ were synthesized by procedures analogous to those described previously.[23,53] SDS-PAGE and silver staining were performed, as described

previously.[23] Procedures detailing the preparation of Aβm$_{17-36}$ and Aβm$_{17-35}$, SDS-PAGE, silver staining, and X-ray crystallography can be found in the Supporting Information.

■ ASSOCIATED CONTENT

Ⓢ Supporting Information

The Supporting Information is available free of charge at https://pubs.acs.org/doi/10.1021/acs.biochem.3c00526.

Procedures for the synthesis of peptides Aβm$_{17-36}$ and Aβm$_{17-35}$; SDS-PAGE and silver staining; crystallization conditions; and X-ray crystallographic data collection, processing, and refinement can be found in the Supporting Information (PDF)

Accession Codes

PDB 8GJD PDB 8GJC

■ AUTHOR INFORMATION

Corresponding Author

James S. Nowick − Department of Chemistry, University of California, Irvine, Irvine, California 92697-2025, United States; ⓞ orcid.org/0000-0002-2273-1029; Email: jsnowick@uci.edu

Authors

Sarah M. Ruttenberg − Department of Chemistry, University of California, Irvine, Irvine, California 92697-2025, United States

Adam G. Kreutzer − Department of Chemistry, University of California, Irvine, Irvine, California 92697-2025, United States; ⓞ orcid.org/0000-0002-9724-6298

Nicholas L. Truex − Department of Chemistry, University of California, Irvine, Irvine, California 92697-2025, United States

Complete contact information is available at:
https://pubs.acs.org/10.1021/acs.biochem.3c00526

Author Contributions

S.M.R., A.G.K., and J.S.N. designed the research. S.M.R. and J.S.N. wrote the paper. S.M.R. and N.L.T. performed peptide synthesis, purification, and characterization. S.M.R., A.G.K., and N.L.T. performed X-ray crystallography. S.M.R. performed SDS-PAGE. All authors read and approved the paper.

Notes

The authors declare no competing financial interest.

■ ACKNOWLEDGMENTS

■ REFERENCES

(1) Maity, S.; Hashemi, M.; Lyubchenko, Y. L. Nano-Assembly of Amyloid β Peptide: Role of the Hairpin Fold. Sci. Rep. 2017, 7 (1), No. 2344, DOI: 10.1038/s41598-017-02454-0.

(2) Rasmussen, J.; Mahler, J.; Beschorner, N.; Kaeser, S. A.; Häsler, L. M.; Baumann, F.; Nyström, S.; Portelius, E.; Blennow, K.; Lashley, T.; Fox, N. C.; Sepulveda-Falla, D.; Glatzel, M.; Oblak, A. L.; Ghetti, B.; Nilsson, K. P. R.; Hammarström, P.; Staufenbiel, M.; Walker, L.

C.; Jucker, M. Amyloid polymorphisms constitute distinct clouds of conformational variants in different etiological subtypes of Alzheimer's disease. *Proc. Natl. Acad. Sci. U.S.A.* **2017**, *114* (49), 13018−13023, DOI: 10.1073/pnas.1713215114.

(3) Tycko, R. Amyloid Polymorphism: Structural Basis and Neurobiological Relevance. *Neuron* **2015**, *86* (3), 632−645.

(4) Abelein, A.; Abrahams, J. P.; Danielsson, J.; Gräslund, A.; Jarvet, J.; Luo, J.; Tiiman, A.; Wärmländer, S. K. The Hairpin Conformation of the Amyloid β Peptide Is an Important Structural Motif along the Aggregation Pathway. *JBIC, J. Biol. Inorg. Chem.* **2014**, *19* (4−5), 623−634.

(5) Ono, K.; Condron, M. M.; Teplow, D. B. Structure−Neurotoxicity Relationships of Amyloid β-Protein Oligomers. *Proc. Natl. Acad. Sci. U.S.A.* **2009**, *106* (35), 14745−14750.

(6) Miller, Y.; Ma, B.; Nussinov, R. Polymorphism in Alzheimer AB Amyloid Organization Reflects Conformational Selection in a Rugged Energy Landscape. *Chem. Rev.* **2010**, *110* (8), 4820−4838.

(7) Lührs, T.; Ritter, C.; Adrian, M.; Riek-Loher, D.; Bohrmann, B.; Döbeli, H.; Schubert, D.; Riek, R. 3D Structure of Alzheimer's Amyloid-β(1−42) Fibrils. *Proc. Natl. Acad. Sci. U.S.A.* **2005**, *102* (48), 17342−17347.

(8) Petkova, A. T.; Yau, W.-M.; Tycko, R. Experimental Constraints on Quaternary Structure in Alzheimer's β-Amyloid Fibrils. *Biochemistry* **2006**, *45* (2), 498−512.

(9) Ciudad, S.; Puig, E.; Botzanowski, T.; Meigooni, M.; Arango, A. S.; Do, J.; Mayzel, M.; Bayoumi, M.; Chaignepain, S.; Maglia, G.; Cianferani, S.; Orekhov, V.; Tajkhorshid, E.; Bardiaux, B.; Carulla, N. AB(1−42) Tetramer and Octamer Structures Reveal Edge Conductivity Pores as a Mechanism for Membrane Damage. *Nat. Commun.* **2020**, *11* (1), No. 3014, DOI: 10.1038/s41467-020-16566-1.

(10) Wu, J.; Blum, T. B.; Farrell, D. P.; DiMaio, F.; Abrahams, J. P.; Luo, J. Cryo-Electron Microscopy Imaging of Alzheimer's Amyloid-Beta 42 Oligomer Displayed on a Functionally and Structurally Relevant Scaffold. *Angew. Chem., Int. Ed.* **2021**, *60* (34), 18680−18687.

(11) Morimoto, A.; Irie, K.; Murakami, K.; Masuda, Y.; Ohigashi, H.; Nagao, M.; Fukuda, H.; Shimizu, T.; Shirasawa, T. Analysis of the Secondary Structure of β-Amyloid (AB42) Fibrils by Systematic Proline Replacement. *J. Biol. Chem.* **2004**, *279* (50), 52781−52788.

(12) Masuda, Y.; Uemura, S.; Ohashi, R.; Nakanishi, A.; Takegoshi, K.; Shimizu, T.; Shirasawa, T.; Irie, K. Identification of Physiological and Toxic Conformations in AB42 Aggregates. *ChemBioChem* **2009**, *10* (2), 287−295.

(13) Hoyer, W.; Grönwall, C.; Jonsson, A.; Ståhl, S.; Härd, T. Stabilization of a β-Hairpin in Monomeric Alzheimer's Amyloid-β Peptide Inhibits Amyloid Formation. *Proc. Natl. Acad. Sci. U.S.A.* **2008**, *105* (13), 5099−5104.

(14) Sonar, K.; Mancera, R. L. Characterization of the Conformations of Amyloid Beta 42 in Solution That May Mediate Its Initial Hydrophobic Aggregation. *J. Phys. Chem. B* **2022**, *126* (40), 7916−7933.

(15) Liu, P.; Reed, M. N.; Kotilinek, L. A.; Grant, M. K. O.; Forster, C. L.; Qiang, W.; Shapiro, S. L.; Reichl, J. H.; Chiang, A. C. A.; Jankowsky, J. L.; Wilmot, C. M.; Cleary, J. P.; Zahs, K. R.; Ashe, K. H. Quaternary Structure Defines a Large Class of Amyloid-β Oligomers Neutralized by Sequestration. *Cell Rep.* **2015**, *11* (11), 1760−1771.

(16) Benilova, I.; Karran, E.; De Strooper, B. The Toxic AB Oligomer and Alzheimer's Disease: An Emperor in Need of Clothes. *Nat. Neurosci.* **2012**, *15* (3), 349−357.

(17) Cline, E. N.; Bicca, M. A.; Viola, K. L.; Klein, W. L. The Amyloid-β Oligomer Hypothesis: Beginning of the Third Decade. *J. Alzheimer's Dis.* **2018**, *64* (s1), S567−S610. DOI: 10.3233/JAD-179941.

(18) Lendel, C.; Bjerring, M.; Dubnovitsky, A.; Kelly, R. T.; Filippov, A.; Antzutkin, O. N.; Nielsen, N. C.; Härd, T. A hexameric peptide barrel as building block of amyloid-β Protofibrils. *Angew. Chem., Int. Ed.* **2014**, *53*, 12756−12760.

(19) Sandberg, A.; Luheshi, L. M.; Söllvander, S.; Pereira de Barros, T.; Macao, B.; Knowles, T. P.; Biverstål, H.; Lendel, C.; Ekholm-Petterson, F.; Dubnovitsky, A.; Lannfelt, L.; Dobson, C. M.; Härd, T. Stabilization of Neurotoxic Alzheimer Amyloid-β Oligomers by Protein Engineering. *Proc. Natl. Acad. Sci. U.S.A.* **2010**, *107* (35), 15595−15600.

(20) Wang, Y.; Truex, N. L.; Vo, N. D. P.; Nowick, J. S. Effects of Charge and Hydrophobicity on the Oligomerization of Peptides Derived from IAPP. *Bioorg. Med. Chem.* **2018**, *26* (6), 1151−1156.

(21) Kreutzer, A. G.; Nowick, J. S. Elucidating the Structures of Amyloid Oligomers with Macrocyclic β-Hairpin Peptides: Insights into Alzheimer's Disease and Other Amyloid Diseases. *Acc. Chem. Res.* **2018**, *51* (3), 706−718.

(22) Samdin, T. D.; Wierzbicki, M.; Kreutzer, A. G.; Howitz, W. J.; Valenzuela, M.; Smith, A.; Sahrai, V.; Truex, N. L.; Klun, M.; Nowick, J. S. Effects of N-Terminal Residues on the Assembly of Constrained β-Hairpin Peptides Derived from AB. *J. Am. Chem. Soc.* **2020**, *142* (26), 11593−11601.

(23) Guaglianone, G.; Kreutzer, A. G.; Nowick, J. S.Synthesis and Study of Macrocyclic β-Hairpin Peptides for Investigating Amyloid Oligomers. In *Synthetic and Enzymatic Modifications of the Peptide Backbone*; Elsevier, 2021; Vol. *656*, pp 123−168 DOI: 10.1016/bs.mie.2021.04.023.

(24) Samdin, T. D.; Kreutzer, A. G.; Nowick, J. S. Exploring Amyloid Oligomers with Peptide Model Systems. *Curr. Opin. Chem. Biol.* **2021**, *64*, 106−115.

(25) Howitz, W. J.; Guaglianone, G.; McKnelly, K. J.; Haduong, K.; Ashby, S. N.; Laayouni, M.; Nowick, J. S. Macrocyclic Peptides Derived from Familial Alzheimer's Disease Mutants Show Charge-Dependent Oligomeric Assembly and Toxicity. *ACS Chem. Neurosci.* **2022**, *13* (6), 714−720, DOI: 10.1021/acschemneuro.1c00833.

(26) McKnelly, K. J.; Kreutzer, A. G.; Howitz, W. J.; Haduong, K.; Yoo, S.; Hart, C.; Nowick, J. S. Effects of Familial Alzheimer's Disease Mutations on the Assembly of a β-Hairpin Peptide Derived from AB16−36. *Biochemistry* **2022**, *61* (6), 446−454.

(27) Liu, C.; Sawaya, M. R.; Cheng, P.-N.; Zheng, J.; Nowick, J. S.; Eisenberg, D. Characteristics of Amyloid-Related Oligomers Revealed by Crystal Structures of Macrocyclic β-Sheet Mimics. *J. Am. Chem. Soc.* **2011**, *133* (17), 6736−6744.

(28) Bitan, G.; Kirkitadze, M. D.; Lomakin, A.; Vollers, S. S.; Benedek, G. B.; Teplow, D. B. Amyloid β-Protein (AB) Assembly: AB40 and AB42 Oligomerize through Distinct Pathways. *Proc. Natl. Acad. Sci. U.S.A.* **2003**, *100* (1), 330−335.

(29) Pujol-Pina, R.; Vilaprinyó-Pascual, S.; Mazzucato, R.; Arcella, A.; Vilaseca, M.; Orozco, M.; Carulla, N. SDS-PAGE Analysis of AB Oligomers Is Disserving Research into Alzheimer's Disease: Appealing for ESI-Im-MS. *Sci. Rep.* **2015**, *5* (1), No. 14809, DOI: 10.1038/srep14809.

(30) Kreutzer, A. G.; Samdin, T. D.; Guaglianone, G.; Spencer, R. K.; Nowick, J. S. X-Ray Crystallography Reveals Parallel and Antiparallel β-Sheet Dimers of a β-Hairpin Derived from AB16−36 That Assemble to Form Different Tetramers. *ACS Chem. Neurosci.* **2020**, *11* (15), 2340−2347.

(31) Zhang, S.; Yoo, S.; Snyder, D. T.; Katz, B. B.; Henrickson, A.; Demeler, B.; Wysocki, V. H.; Kreutzer, A. G.; Nowick, J. S. A Disulfide-Stabilized Aβ That Forms Dimers but Does Not Form Fibrils. *Biochemistry* **2022**, *61* (4), 252−264.

(32) We believe that this treatment leads to the transient formation of covalently bonded oligomers HS-Aβ-S-(PR$_3$-S-Aβ-S)$_n$-Aβ-SH

(33) Kreutzer, A. G.; Yoo, S.; Spencer, R. K.; Nowick, J. S. Stabilization, Assembly, and Toxicity of Trimers Derived from AB. *J. Am. Chem. Soc.* **2017**, *139* (2), 966−975.

(34) Kreutzer, A. G.; Spencer, R. K.; McKnelly, K. J.; Yoo, S.; Hamza, I. L.; Salveson, P. J.; Nowick, J. S. A hexamer of a peptide derived from AB16−36. *Biochemistry* **2017**, *56* (45), 6061−6071.

(35) Laganowsky, A.; Liu, C.; Sawaya, M. R.; Whitelegge, J. P.; Park, J.; Zhao, M.; Pensalfini, A.; Soriaga, A. B.; Landau, M.; Teng, P. K.; Cascio, D.; Glabe, C.; Eisenberg, D. Atomic View of a Toxic Amyloid

Small Oligomer. *Science* **2012**, *335* (6073), 1228−1231, DOI: 10.1126/science.1213151.

(36) The crystal structure of peptide 1a which contains the mutation M35O, further emphasizes the lack of involvement of residue 35 in this assembly (Figure S#). Trimers and hexamers formed by peptides 1 and 1a are almost identical—the α-linked ornithine residue is situated similarly to the methionine it replaces, and neither contributes to the hydrophobic packing at the core of the hexamers

(37) Shao, H.; Jao, S.-c.; Ma, K.; Zagorski, M. G. Solution Structures of Micelle-Bound Amyloid β-(1−40) and β-(1−42) Peptides of Alzheimer's Disease 1 1edited by P. E. Wright. *J. Mol. Biol.* **1999**, *285* (2), 755−773.

(38) Jarvet, J.; Danielsson, J.; Damberg, P.; Oleszczuk, M.; Gräslund, A. Positioning of the Alzheimer AB(1−40) Peptide in SDS Micelles Using NMR and Paramagnetic Probes. *J. Biomol. NMR* **2007**, *39* (1), 63−72.

(39) Mandal, P. K.; Pettegrew, J. W. Alzheimer's Disease: Soluble Oligomeric aβ(1−40) Peptide in Membrane Mimic Environment from Solution NMR and Circular Dichroism Studies. *Neurochem. Res.* **2004**, *29* (12), 2267−2272.

(40) Terzi, E.; Hölzemann, G.; Seelig, J. Interaction of Alzheimer β-Amyloid Peptide(1−40) with Lipid Membranes. *Biochemistry* **1997**, *36* (48), 14845−14852.

(41) de Planque, M. R. R.; Raussens, V.; Contera, S. A.; Rijkers, D. T. S.; Liskamp, R. M. J.; Ruysschaert, J.-M.; Ryan, J. F.; Separovic, F.; Watts, A. B-Sheet Structured β-Amyloid(1−40) Perturbs Phosphatidylcholine Model Membranes. *J. Mol. Biol.* **2007**, *368* (4), 982−997.

(42) Lau, T.-L.; Ambroggio, E. E.; Tew, D. J.; Cappai, R.; Masters, C. L.; Fidelio, G. D.; Barnham, K. J.; Separovic, F. Amyloid-β Peptide Disruption of Lipid Membranes and the Effect of Metal Ions. *J. Mol. Biol.* **2006**, *356* (3), 759−770.

(43) Dahse, K.; Garvey, M.; Kovermann, M.; Vogel, A.; Balbach, J.; Fändrich, M.; Fahr, A. DHPC Strongly Affects the Structure and Oligomerization Propensity of Alzheimer's AB(1−40) Peptide. *J. Mol. Biol.* **2010**, *403* (4), 643−659.

(44) Rangachari, V.; Reed, D. K.; Moore, B. D.; Rosenberry, T. L. Secondary Structure and Interfacial Aggregation of Amyloid-β(1−40) on Sodium Dodecyl Sulfate Micelles. *Biochemistry* **2006**, *45* (28), 8639−8648.

(45) Lindberg, D. J.; Wesén, E.; Björkeroth, J.; Rocha, S.; Esbjörner, E. K. Lipid Membranes Catalyse the Fibril Formation of the Amyloid-β (1−42) Peptide through Lipid-Fibril Interactions That Reinforce Secondary Pathways. *Biochim. Biophys. Acta, Biomembr.* **2017**, *1859* (10), 1921−1929.

(46) Petkova, A. T.; Buntkowsky, G.; Dyda, F.; Leapman, R. D.; Yau, W.-M.; Tycko, R. Solid State NMR Reveals a Ph-Dependent Antiparallel β-Sheet Registry in Fibrils Formed by a β-Amyloid Peptide. *J. Mol. Biol.* **2004**, *335* (1), 247−260.

(47) Kusumoto, Y.; Lomakin, A.; Teplow, D. B.; Benedek, G. B. Temperature Dependence of Amyloid β-Protein Fibrillization. *Proc. Natl. Acad. Sci. U.S.A.* **1998**, *95* (21), 12277−12282.

(48) Niu, Z.; Zhang, Z.; Zhao, W.; Yang, J. Interactions between Amyloid β Peptide and Lipid Membranes. *Biochim. Biophys. Acta, Biomembr.* **2018**, *1860* (9), 1663−1669.

(49) Rangachari, V.; Moore, B. D.; Reed, D. K.; Sonoda, L. K.; Bridges, A. W.; Conboy, E.; Hartigan, D.; Rosenberry, T. L. Amyloid-β(1−42) Rapidly Forms Protofibrils and Oligomers by Distinct Pathways in Low Concentrations of Sodium Dodecylsulfate. *Biochemistry* **2007**, *46* (43), 12451−12462.

(50) Rangachari, V.; Dean, D. N.; Rana, P.; Vaidya, A.; Ghosh, P. Cause and Consequence of AB − Lipid Interactions in Alzheimer Disease Pathogenesis. *Biochim. Biophys. Acta, Biomembr.* **2018**, *1860* (9), 1652−1662.

(51) Ege, C.; Lee, K. Y. Insertion of Alzheimer's AB40 Peptide into Lipid Monolayers. *Biophys. J.* **2004**, *87* (3), 1732−1740.

(52) In ion-mobility mass spectrometry (IM-MS), the peptides remained monomeric in both the presence and absence of the nonionic detergent DDM. Analytical ultracentrifugation (AUC) was attempted in the presence and absence of SDS, but did not provide clear insights into the assembly states of the peptides.

(53) iPSC-derived cortical neurons were treated with up to 50 μM of either peptide for 72 h. Neither peptide exhibited toxicity by Promega assays CellTiter-Glo Luminescent Cell Viability Assay and CytoTox-Glo Cytotoxicity Assay (data not shown).